TECHNICAL MEMORANDUMS

NATIONAL ADVISORY COMMITTEE FOR AERONAUTICS

No. 880

THE EFFECTIVE WIDTH OF CURVED SHEET AFTER BUCKLING

By W. A. Wenzek

Luftfahrtforschung
Vol. 15, No. 7, July 6, 1938
Verlag von R. Oldenbourg, München und Berlin

Washington
November 1938

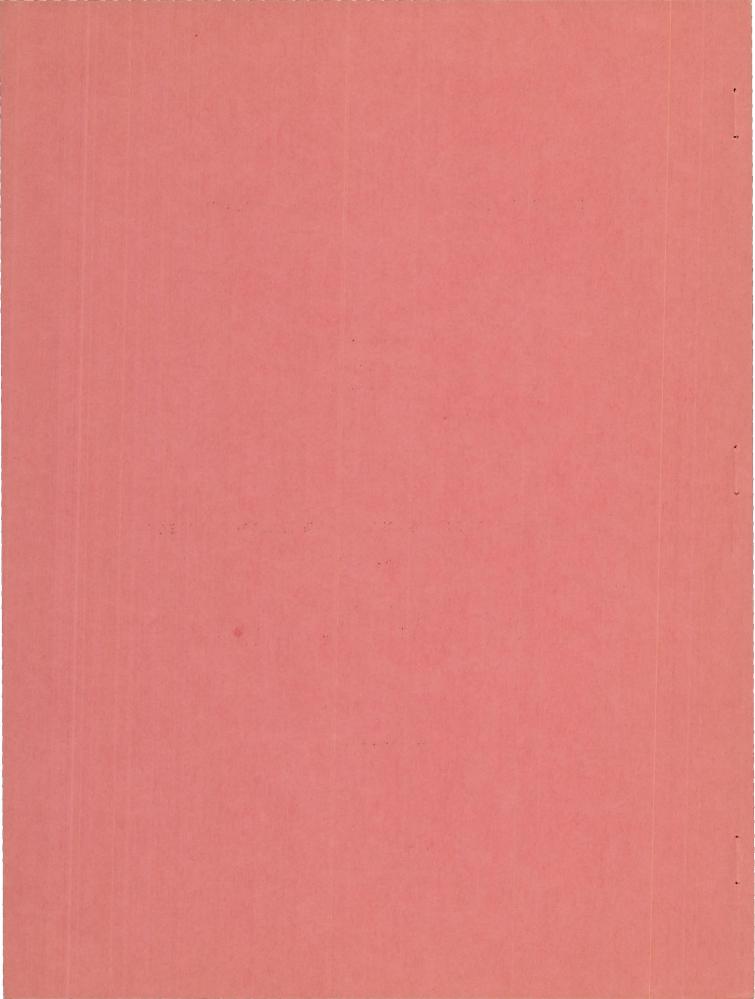NATIONAL ADVISORY COMMITTEE FOR AERONAUTICS

TECHNICAL MEMORANDUM NO. 880

THE EFFECTIVE WIDTH OF CURVED SHEET AFTER BUCKLING*

By W. A. Wenzek

SUMMARY

The present report contains a description of experiments made for the purpose of ascertaining the effective width of circularly curved sheet under pure flexural stress.

A relation for the effective width of curved sheets is established. Comparisons with similar tests made by the DVL manifest good agreement.

I. INTRODUCTION

Experiments were made with circular cylinders compressed in longitudinal direction. The sheets were rigidly built in at the sides parallel to the axis of the cylinder. This should be borne in mind when applying the results to constructed airplane shells since frequently during riveting or by wide rivet pitch the sheet buckles at the stiffener sections also.

In stiffened shells under compression the carrying capacity of the buckled sheet between stiffeners can be accounted for by the introduction of an "effective width." The sheet is replaced by two assumedly buckling-resistant sheet strips of such width $2 b_R$, that their carrying capacity under a stress equivalent to the shortening at the sheet edge is the same as that of the buckled sheet panel (fig. 1). For sheets rigidly built in at the side this stress is equal to the edge stress σ_R of the sheet.

$$\sigma_R \, 2 \, b_R = \sigma_m \, t \qquad (1)$$

To find the carrying capacity or the effective width $2\,b_R$, respectively, circular brass cylinders were tested in pure compression conformably to figure 2. From the total load and the shortening of the section measured during the test, the section load (with allowance for the section shares) and the effective width of the sheet were obtained.

With unsymmetrically arranged stiffener sections which, aside from compression, are also subjected to small flexural stresses - say, due to eccentrically applied load for instance - the edge stress σ_R and the mean section stress σ_{m_P} manifest considerable discrepancies under certain circumstances. In such cases, it is preferable to refer the value for the effective width for practical reasons by $\dfrac{\sigma_R}{\sigma_{m_P}}$ to the mean section stress:

$$2\,b_{m_P} = \frac{\sigma_R}{\sigma_{m_P}} \, 2\,b_R = F_1\left(\frac{\sigma_R}{\sigma_k}\right) F_2\left(\frac{\sigma_R}{\sigma_k}\right) \tag{2}$$

II. RESULTS

The effective width of the flat sheet in pure compression is, according to Lahde-Wagner (reference 1)

$$\frac{2\,b_R}{t} = k\sqrt{\frac{\sigma_k}{\sigma_R}} \tag{3}$$

whereby a slightly exceeded buckling stress $\left(\dfrac{\sigma_R}{\sigma_k} < 3\right)$ is presumed for $k = 1$. By considerably exceeded buckling stress $\left(\dfrac{\sigma_R}{\sigma_k} > 3\right)$ k ultimately approaches 2. The factor k was obtained from experiments on sheets with rigidly built-in edges.

On the basis of these tests, the equation for the effective width of circularly curved sheets is as follows

$$\frac{2\,b_R}{t} = \sqrt{\frac{\sigma_k}{\sigma_R}} - \varphi\left(1 - \frac{\sigma_k}{\sigma_R}\right) \tag{4}$$

where $\varphi = \dfrac{t}{r}$ is the angle at center of the sheet panel,

$\sigma_R,$ the edge stress appearing at the edge of the sheet, and

$$\sigma_k = \sigma_{e_b} + \sigma_{kr} = 5\,E\left(\frac{s}{t}\right)^2 + 0.3\,E\left(\frac{s}{r}\right) \quad \text{is the}$$

buckling stress of the panel.

The values for $\dfrac{2\,b_R}{t}$ are plotted in figure 3 for the

flat sheet according to equation (3) and for the curved sheet (φ up to 30°) according to equation (4) against

the degree of exceeded buckling load $\left(\dfrac{\sigma_R}{\sigma_k} \text{ up to } 13\right)$.

In the extreme case of $\varphi = 0$, equation (4) becomes equation (3) for the flat sheet provided that the buckling

stress is not substantially exceeded $\left(\dfrac{\sigma_R}{\sigma_k} < 3, \text{ i.e.,}\right.$

$\left. k = 1\right)$. Otherwise $\left(\dfrac{\sigma_R}{\sigma_k} > 3\right)$ we find $k > 1$ for the

flat sheet according to Wagner-Lahde's tests; and in this case the curved sheet, equation (4) does not change to the flat sheet, equation (3). Within the zone of very small φ rigidly built-in sheets probably disclose marked sensitivity relative to original curvatures.

Equation (4) is applicable to sheets with built-in longitudinal edges under pure compression. For the panel edge diagonal to the direction of compression, the experiments disclosed no noticeable impairment of the wrinkling condition as a result of the clamping effect, on tolerably great panel length l to panel width t ($l/t > 2.5$).

With regard to the range of the dimensions, equation (4) applies only to such dimensioned sheets as at buckling manifest elastic strains.

Figure 4 illustrates the results of a calculation of the effective width for the same edge stresses according to equation (4) plotted against the angle at the center φ. The data refer to brass sheets of given aspect ratio $\left(\dfrac{t}{s} = 500\right)$. The effective width grows, as is seen, almost proportionally with φ in the plotted range. Only at high

edge stresses does an almost complete flattening-out of
the lines take place. A means of comparison between the
carrying capacity of flat ($\varphi = 0$) and curved sheet is
afforded by the dashed line; its location complies with
the condition $2\ b_{R(curved)} = 2\ b_{R(flat)}$.

III. TEST SPECIMENS AND TEST LAY-OUT

Altogether, eleven test cylinders of springy sheet
brass* were provided.   The panels were riveted together
by copper rivets with a 2 cm pitch at the lap-riveted
seams and 3 cm at the sections (fig. 2). Against undesir-
able wrinkling of the sheet edge a symmetrical arrangement
of the flanged sections and flattened sheet edges provided
in some measure a guarantee for the zones of maximum com-
pression stress as well. To forestall an adverse load
initiation, the test specimen and the pressure plate of the
experimental set-up were mutually fitted in to about 7/1000
mm under light-slot control by luminous bodies mounted in
the cylinder.

The choice of cylinder dimensions was largely governed
by the customary range of application in airplane shell con-
struction.

Table I contains the most important cylinder dimen-
sions, the individual φ, $\dfrac{r}{s}$, and $\dfrac{t}{s}$ values as well as
cross-section proportions of section and sheet, along with
the theoretical and experimental buckling-stress data.

The test lay-out (fig. 5) consists of two pressure
plates whose distance can be varied as desired by a spindle.
To assure purest possible compression stresses, a flexible
tension bar a was mounted at the lower end of the spindle
and the lower pressure plate was fitted with a longitudinal
ball bearing. The test load was computed from the measured
sag of two springs c mounted on knife edges b, figure 6.
The instrumental accuracy was around 1 percent within the
range of 600 to 10,000 kg.

---

*Elongation (strain) measurements on cylinders 4, 6, 7, and
8 averaged $E = 1.03 \times 10^6$ kg/cm², and $E = 1.06 \times 10^6$
kg/cm² for the others.

IV. TEST PROCEDURE AND INTERPRETATION

The test cylinders were progressively loaded to failure, i.e., to the highest admissible stress of the test lay-out. The compressive strain ϵ_P in the sections was recorded on three dial gages (figs. 8 to 12). The readings were simultaneous and afforded good agreement before and after buckling.

The evaluation of the measurements was as follows: from the difference of total load P_G and section load $P_P = 3 \, \epsilon \, E \, F_P$ the load supported by the sheet was obtained after which with consideration to the sheet area $F_B = 3 \, s \, t$ the effective width was computed at

$$2 \, b_R = \frac{3 \, P_B \quad 3 \, F_P}{3 \, P_P \quad 3 \, F_B} \, t$$

Figure 7 illustrates the test data for the effective width arranged according to φ. The experimentally defined values for $\dfrac{2 \, b_R}{t}$ (single dots) and those computed according to equation (4) (solid line) are shown plotted against the degree of exceeded theoretical buckling load $\left(\dfrac{\sigma_R}{\sigma_k} \right)$.

a) Buckling Stress of Sheet Panel

Buckling occurred simultaneously on all three panels. The experimental buckling stresses are in good agreement with the theoretical values

$$\left(\sigma_k = \sigma_{e_b} + \sigma_{kr} = 5 \, E \left(\frac{s}{t} \right)^2 + 0.3 \, E \, \frac{s}{r} \right)$$

except for cylinders 9, 10, and 11, with large φ, where the experimental exceeded the calculated figures by as much as 35 percent.

b) Wrinkling and Carrying Capacity

Small φ ($\varphi = 2.5°$, $5°$, $3.5°$) were accompanied by ar-

bitrary oppositely staggered wrinkles. With increasingly
exceeding critical stress, secondary buckles, usually
starting at the edge of the sheet, manifested themselves.
Further increasing edge stress was followed by sudden
bulge rearrangement accompanied by a reduction in effec-
tive width, as illustrated in figure 7 for cylinders 1 and

2 at $\frac{\sigma_R}{\sigma_k} = 7.5$ and $= 5$, respectively. The test values

for both cylinders is on the average in good agreement with
equation (4) and very good for cylinder 3.

At medium $\varphi (\varphi = 13^\circ$ and $30^\circ)$ and slightly exceeded
buckling stress, all panels disclosed only one inwardly
directed bulge, which, however, was also followed by sec-
ondary bulges as the buckling stress was increasingly ex-
ceeded, although to a lesser extent than for the originally
slightly curved sheets (figs. 8 and 9). There was no re-
versal of bulges for $\varphi = 30^\circ$. Cylinder No. 6 disclosing
a comparatively flat course of the effective width, evinced
no secondary bulges even after markedly exceeded buckling
stress. The carrying capacity of cylinders 4, 7, and 8,
with the same φ but different wall thicknesses ($s = 0.036$
cm and $s = 0.052$ cm) showed good agreement with equation (4).

Cylinder No. 5 disclosed a marked reduction in carry-
ing capacity as a result of additional prebulges produced
during riveting, as seen in figure 10 and 11, especially on
the section at the right. They also show their not incon-
siderable effect on the secondary bulges near the edge.

At great φ ($\varphi = 65^\circ$ and 113°) the experiments showed
severe bulging (fig. 12, cylinder No. 11, correspond to
$\varphi = 113^\circ$). As regards the carrying capacity, cylinder No.
10 gave only one test point, while on cylinders Nos. 9 and
11 sheet and section buckled simultaneously.

c) Form of Failure

On all cylinders the failure of the edge section oc-
curred in the plastic range directly adjacent to the prin-
cipal bulges (figs. 10 and 11).

APPENDIX

In the DVL five test specimens (reference 2) (panels) of duralumin with section stiffeners on one side were compressed according to figure 13 over fitted-on clamping rails. The stresses were recorded during the tests at various points of the sheet (σ_R) and on the stiffening sections (σ_{m_P}) with tensiometers according to arrangement in figure 13. The records disclosed additional bending stresses on the sections of all panels.

These DVL tests were also used to check equation (4) The effective width $2\,b_R$ was computed from the DVL data and plotted in figure 14 for comparison with equation (4) (solid curve).

The panels 2, 3, and 4 with different $\frac{l}{t}$ values (2.5 and 5.2) manifest good agreement with equation (4). While panel 5 with outside stiffener sections and especially panel 1 give surprisingly high values for the effective width. In these two panels the supplementary bending stresses were especially high. The discrepancies between the DVL test data and equation (4) is probably traceable to the fact that in connection with this bending the shortening of the panel in the median zone was not the same as that on its edge.

Translation by J. Vanier,
National Advisory Committee
for Aeronautics.

REFERENCES

1. Lahde, R., and Wagner, H.: Experimental Studies of the Effective Width of Buckled Sheets. T.M. No. 814, N.A.C.A., 1936.

2. Ebner, H.: The Strength of Shell Bodies - Theory and Practice. T.M. No. 838, N.A.C.A., 1937.

TABLE I. Dimensions and Buckling Stresses of the Test Cylinders (in cm, kg units)

| Identification		1	2	3	4	5	6	7	3	9	10	11
						Test cylinders						
Angle at center . . . . . φ		2.5°	5°	8.5°	13°	13°	19.5°	30°	30°	65°	66°	113°
Curvature radius. . . . . r		410	248	180	103	120	53	54	57	29	25	17.8
Sheet panel length . . . l		47.4	55.0	57.5	58.5	65.7	45	70	70	82	70	86
width. . . . t		18.7	21.7	27	23.4	27	18	28	30	33	28.8	35
thickness. . s		0.101	0.080	0.062	0.081	0.042	0.072	0.036	0.052	0.045	0.05	0.041
Ratio of . . . . l/t		2.54	2.53	2.5	2.5	2.5	2.5	2.5	2.33	2.49	2.43	2.46
. . . . r/s		4060	3100	2900	1270	2845	730	1500	1090	644	500	430
. . . . t/s		185	270	435	289	643	250	780	577	730	576	355
Thickness of section. . . s_s		0.062	0.061	0.042	0.062	0.031	0.050	0.030	0.035	0.035	0.035	0.035
Total area of cylinder. . F_Z		8.73	8.04	6.85	8.62	4.92	6.36	4.32	6.4	5.1	6.06	5.98
Proportion of sheet in percent of . F_Z		64.8	64.9	69.7	66.3	70.3	62.1	70.8	73.1	73.4	72.2	72.6
Proportion of section in percent of		35.2	35.1	30.3	33.7	29.7	37.9	29.2	26.9	26.6	27.8	27.4
Buckling stress of flat sheet. . . . . σ_{eb}		155	73	26	62	13	83	9	16	10	16	7
Increase in stress due to curvature . . . . . σ_{kr}		78	103	110	244	109	423	206	284	493	636	738
Buckling stress of curved sheet . . . . . σ_K		233	176	136	306	122	506	215	300	503	652	745
Experimentally defined buckling stress. . . σ_{Kv}		220	170	107	370	131	560	190	320	660	820	800
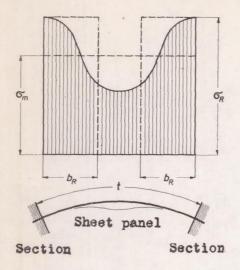
Figure 1.- Stress distribution over panel width t.
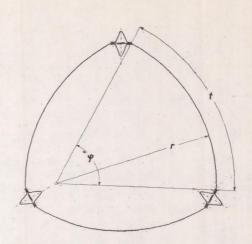
Figure 2.- Section of a test cylinder.
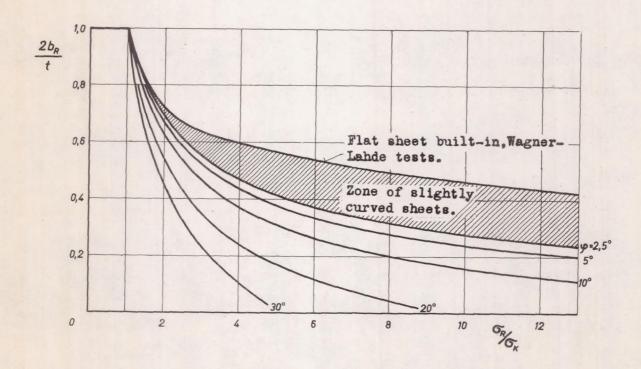
Figure 3.- The effective width for flat and circular curved
            sheets plotted against the degree of exceeded
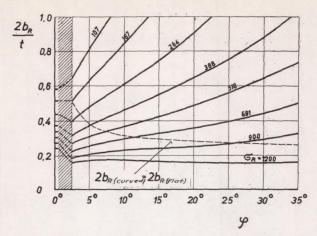   buckling stress (nondimensional presentation).

Figure 4.- The effective width for identical edge stresses
plotted against φ (ratio of sheet width to wall
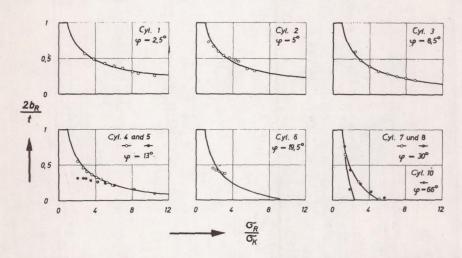thickness: $\frac{t}{s} = 500$, (material: brass).

Figure 7.- Test data for the effective width arranged
according to φ.
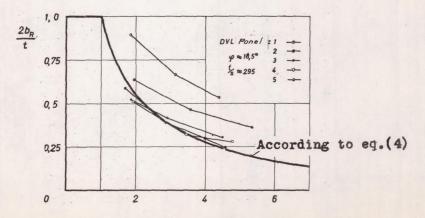
Figure 14.- Comparison of the DVL data with the data
for the effective width according to eq.(4).

Flexible
tension rod.
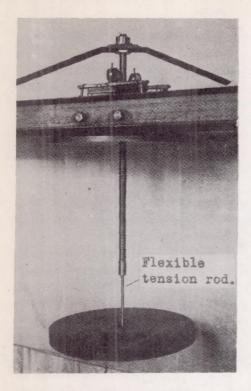
Figure 5.- Test arrangement.
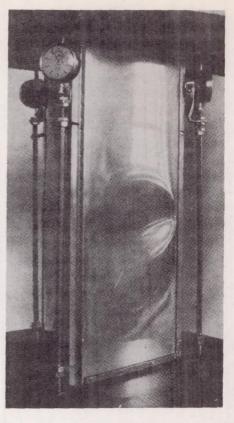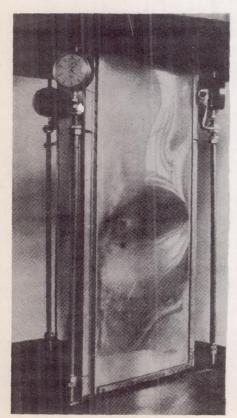
Figure 8.- Test cylinder   no.4
at $\sigma_R/\sigma_K = 2.48$

Figure 6.- Setup for determining
the test load.
b — Knife edges.
Springs c mounted on b.

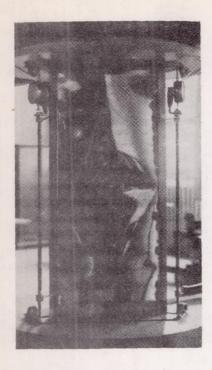Figure 9.- Test cylinder   no.4
at $\sigma_R/\sigma_K = 5$.

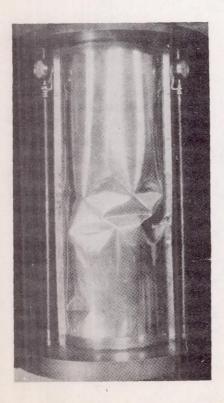Figure 10.- Test cylinder no.5
at $\sigma_R/\sigma_K = 4.63$

Figure 11.- Test cylinder no.5
(form of failure)
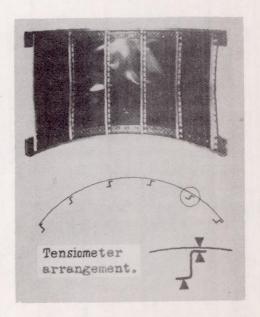
Figure 13.- DVL test arrangement.

Figure 12.- Test cylinder no.11
(form of failure)